Desiccation and shrinkage properties of slurry clay with crack development

Hikaru Seya[1], T. Umezaki[2], and T. Kawamura[2]

[1] Interdisciplinary Graduate School of Science and Technology, Shinshu University, 4-17-1, Wakasato, Nagano City 380-8553, Japan.
[2] Faculty of Engineering, Shinshu University, 4-17-1, Wakasato, Nagano City 380-8553, Japan.

ABSTRACT

In order to investigate the characteristics of desiccation shrinkage and crack development in slurry clays, two types of samples with different bubble size distributions were prepared through 'stirring' under atmospheric/vacuum pressure. The inner bubbles and cracks in the specimen were observed through X-ray CT imaging, and the desiccation and volume shrinkage in samples with different initial water content and bubble sizes were evaluated. The main conclusions are as follows. Visible bubbles influence the form of cracks. In spite of the changes in surface area, the rates at which the mass and volume decrease are almost constant from the beginning of drying. Visible bubbles and cracks do not alter the change of water content of the specimen. The relationships w–e and w–S_r and value of e at the end of drying differ depending on visible bubbles.

Keywords: slurry clay; X-ray CT scanner; desiccation crack; water content; void ratio; degree of saturation

1 INTRODUCTION

Volume changes as slurry clay dries involve considerable shrinkage and formation of cracks. In paddy fields and irrigation ponds, the development of desiccation cracks reduces the reservoir capacity. Furthermore, when cracks are generated on a clayey slope, rainwater infiltration into the lower layer can increase the risk of slope failure. Therefore, it is important to investigate the characteristics of desiccation shrinkage and crack development in slurry clays. Umezaki and Kawamura (2013) have proposed the formulation about the shrinkage properties during desiccation of reconstituted cohesive clay as prior research.

In this paper, the authors detail the results of experiments where slurry clay samples with different bubble size distributions were obtained through two preparation methods by 'stirring' under atmospheric/vacuum pressure. These specimens were then air-dried in a plastic greenhouse (Fig. 1). The volume of the specimen during desiccation was calculated using X-ray CT images, and the images were also examined to identify the inner bubbles and cracks in the specimen. These data allowed determining the characteristics of desiccation and volume shrinkage in slurry clay samples with different initial water content and bubble size distributions.

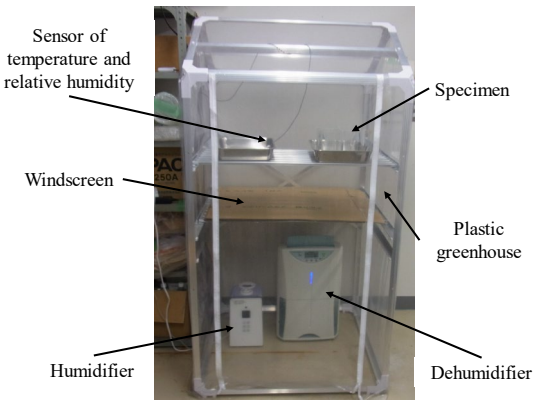

Fig. 1. Test equipment.

2 AIR-DRY TEST OF SLURRY CLAY

Tests were performed on NSF(C) clay samples (soil particle density ρ_S = 2.723 g/cm^3, liquid limit w_L = 57.5%, plastic limit w_P = 35.7% and shrinkage limit w_S = 37.6%) for the test cases listed in Table 1. All tests were conducted in a thermostatic chamber at a room air temperature of 24°C. 70 g of clay powder was used in every case, and deionized water was prepared on the basis of the desired initial water content, w_i. 'Atmospheric-stirred' slurry clay samples were prepared by stirring for 5 min under atmospheric conditions in a 100 mm diameter acrylic container, and 'vacuum-stirred' slurry clay samples were prepared by stirring for 30 min at vacuum pressure (p_v = −97 kPa) in a vacuum chamber. The acrylic container containing sample was then covered with plastic wrap and placed in the plastic greenhouse shown in Fig. 1 for three days. The plastic greenhouse contained a humidifier and a dehumidifier. In order to reduce the influence of wind from the dehumidifier, a sheet of cardboard was set up as a windscreen between it and the specimen. Only the humidifier was operated during sample preparation, and high relative humidity (RH = 70%) was maintained. Before starting the air-dry test, supernatant water on the

Table 1. Test cases

Case	Stirring condition	Initial and starting water content, w_i and w_0	Starting degree of saturation S_{r0}	Starting height, h_0
1	Vacuum pressure	350%, 268.0%	*108.7%	2.43 mm
2		200%, 194.7%	*104.8%	1.90 mm
3		100%, 101.2%	102.0%	1.02 mm
4	Atmospheric pressure	350%, 252.8%	*106.5%	2.38 mm
5		200%, 177.2%	*100.7%	1.87 mm
6		100%, 100.7%	90.9%	1.28 mm

*The calculated values of S_{r0} are slightly larger than in reality.

surface of the sample was removed by suctioning using dropper, resulting in different starting water content, w_0, for test cases with same w_i, as shown in Table 1. However, in Cases 3 and 6, which have lower w_i, there was no supernatant water on the sample, so the value of w_0 was almost equal. The starting degree of saturation, S_{r0}, and height of the specimen, h_0, are given in Table 1. In Cases 1, 2, 4, and 5, supernatant water could not be removed completely. Therefore, the values of S_{r0} in Table 1 are larger than the actual values. The specimen in Case 5 is considered unsaturated condition.

Air-dry tests were conducted by operating only the dehumidifier. In order to calculate w of the specimen during the test, the specimen was removed from the plastic greenhouse approximately every 12 h. The mass of the specimen was measured with an electronic balance with an accuracy of 0.01 g and w was calculated. X-ray CT images were obtained with an X-ray CT scanner (RF Co., Ltd., Japan, computerised tomography scanning equipment NAOMi-CT). X-ray CT sectional views were obtained with NAOMi-CT viewer software (RF Co., Ltd.), as shown in Fig. 2. Horizontal sectional images were outputted for every 202.55 µm in height. Image-analysis software Move-tr/2D (Library Co., Ltd., Japan) was used to calculate the area of the specimen in each horizontal section through pixel counting. The volume of the specimen was calculated using the sectional area and the height of the section. By using the volume of specimen and the mass change due to drying, the values of degree of saturation, S_r, was calculated. Moreover, in order to investigate the horizontal distribution of w during the air-drying process, in addition to the six test cases shown in Table 1, some air-dry tests were stopped after a fixed time had elapsed, the samples were divided into several segments, and the value of w was measured in these.

3 TEST RESULTS AND DISCUSSIONS

Table 2 shows X-ray CT images at h = 2 mm before and after each test. The shade is darker at the center of each specimen because of the attenuation of X-rays as they pass through the specimen. In the 'atmospheric –stirred' specimen, Cases 5 and 6, black spots signifying bubbles are seen more remarkable, as w_i become lower. The visible bubbles did not disappear

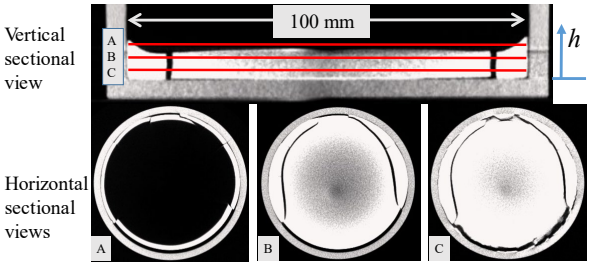

Fig. 2. An example of the sectional views of X-ray CT image

despite the presence of supernatant water on the specimen for three-day preparation. The visible bubbles were confirmed from the specimen after the end of the tests. Furthermore, more cracks with complex geometries form in these cases. Cracks passing through visible bubbles can be observed in Case 6 containing large babbles, indicating that the bubbles influence the form of the cracks. In Case 4 with high water content, visible bubbles were not seen, cracks across the specimen did not generate. In 'atmospheric-stirred' specimen with much higher water content, it is thought that cracks passing through the specimen do not generate. Conversely, visible bubbles were not observed in the 'vacuum-stirred' specimens. In Cases 2 and 3, cracks did not form in the specimens. On the other hand, in Case 1, cracks formed through the specimen near the walls of the acrylic container. It depends on cohesion between specimen and wall, and tensile strength of the specimen. The cracks had a simple geometry and smooth margins, unlike the cracks observed in 'atmospheric-stirred' specimen, Case 5 and 6.

Figs. 3(a)–3(e) show an example of time-dependent changes in the temperature, T, and the relative humidity, RH, in the plastic greenhouse and the mass decrement, Δm, water content, w, and volume, V, of the specimen. As shown in Figs. 3(a) and 3(b), T is almost constant at approximately 24°C, and the RH decreases gradually from about 30% to about 20%. Fig. 3(c) shows that the mass of the specimen decreases almost linearly from the beginning of the test, as the amount of water in the specimen becomes smaller, before becoming almost constant. The evaporation rate of water is higher when the surface area is larger. As slurry clay shrinks, the surface area decreases considerably. However, when a clay specimen is divided into several pieces by crack generation, the surface area increases. Moreover, even if cracks do not occur, the surface area is increased by curvature in the top surface. Irrespective of w_i, visible bubbles and change of the surface area, the rate of mass change during air drying is almost constant, with a decrease rate, $v_m = d(\Delta m)/dt$, of approximately 1 g/h. As shown in Fig. 3(d), the value of w_0 in Cases 1 and 4 and in Cases 2 and 5 were different and in Cases 3 and 6 were almost equal as described in Table 1. On the other hand, as shown in Fig.3(e), the values of V at the beginning of test in Cases 1 and 4 and in Cases 2 and 5 were almost equal, and those in Cases 3 and 6 were

Table 2. X-ray CT images at h = 2 mm before and after all tests

	Case 1: Vacuum-stirring, w_0 = 268.0%	Case 2: Vacuum-stirring, w_0 = 194.7%	Case 3: Vacuum-stirring, w_0 = 101.2%
Before	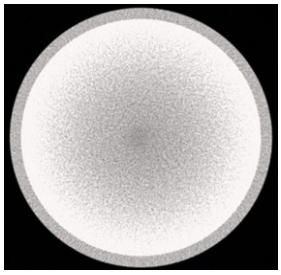	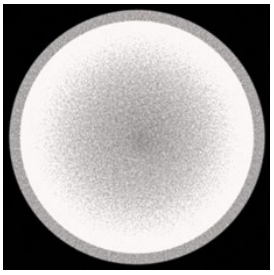	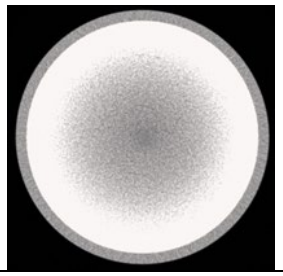
After	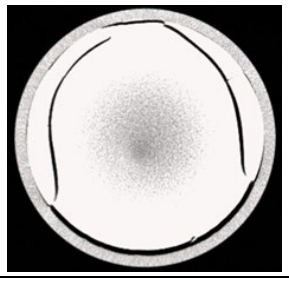		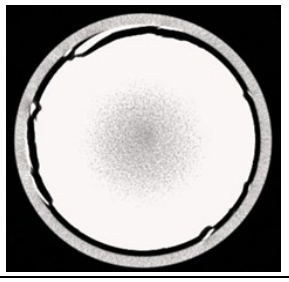
	Case 4: Atmospheric-stirring, w_0 = 252.8%	Case 5: Atmospheric-stirring, w_0 = 177.2%	Case 6: Atmospheric-stirring, w_0 = 100.7%
Before	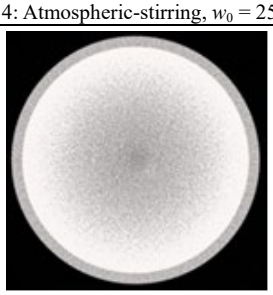	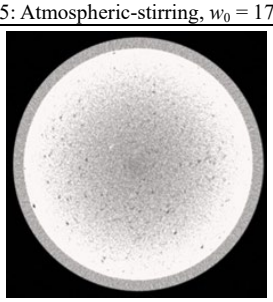	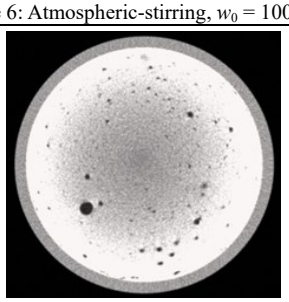
After	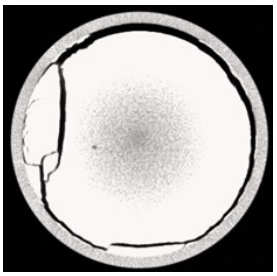	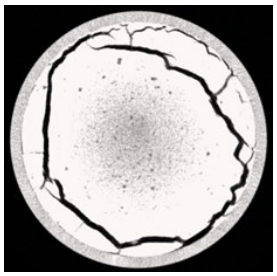	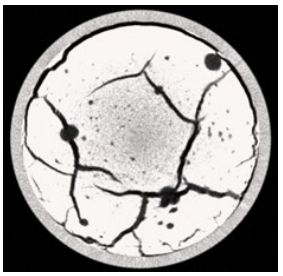

different. These are relevant to the removed supernatant water on the specimen and babbles in the specimen. As shown in Fig. 3(d), w decreases almost linearly and becomes 1-2% at the end of test. Fig. 3(e) shows that the volume of the specimen in all cases decreases linearly from the beginning of the test before reaching a constant value. The rate of decrease in volume becomes also almost constant for all cases independent on w_i, visible bubbles and crack generation. Volume change halts after w decreases to a certain value, prior to the halt in the change in mass.

The horizontal distribution of w in the specimens during air drying is illustrated in Fig. 4. w_n is the actual value of w measured in various parts of a single specimen and $\overline{w}$ is the average value of w_n. w_n was measured for samples collected from the top to the bottom of the specimen evenly. For specimens where there was crack generation, w_n was obtained for various parts, such as the edge of the cracks and the center of the parts divided by cracks. w_n varied from $\overline{w}$ by less than ±1% in all cases. Although the surface area of the specimen changed continuously owing to crack generation during air drying, variations were not seen in the horizontal distribution of w. In every case, $\overline{w}$ is almost equal to the local water content. Visible bubbles and cracks do not alter w.

Figs. 5(a) and 5(b) show the relationships w–S_r and w–e. These relationships follow two patterns. The first one is where there are few visible bubbles in the specimen and no complex cracks are generated, as in Cases 1–4. The other one is where there are numerous visible bubbles in the specimen and complex cracks are generated, as in Cases 5 and 6. Fig. 5(a) shows that, in Cases 1–4, where no complex cracks formed, until the value of w decreased to the value slightly larger than w_S, the value of S_r remained at about 100% irrespective of w_0. As the value of w decreases below the value slightly larger than w_S, the relationship w–S_r becomes linear, decreasing toward the origin. Seya et al. (2017) reported a similar tendency in an air-dry test on fully

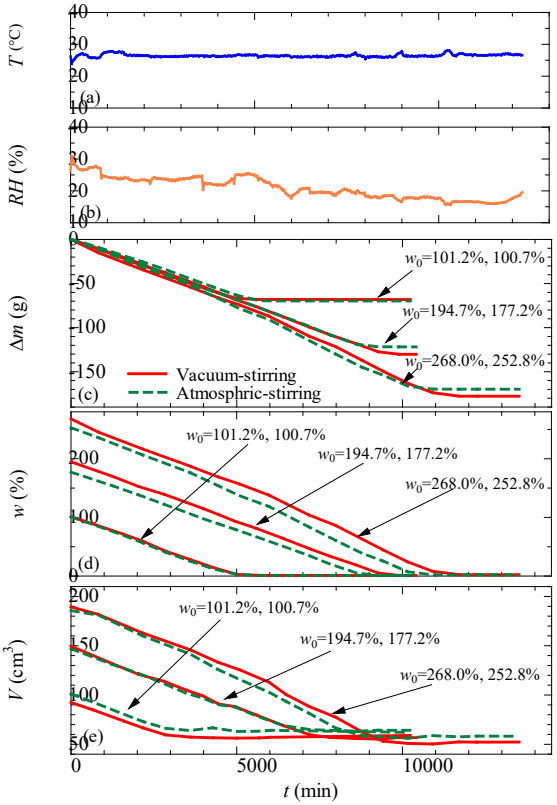

Fig. 3. Test results

deaired slurry clay. On the other hand, in Cases 5 and 6, where there is significant cracking, the value of S_r decreases gradually from around $2w_L$. After it reaches approximately 80%, the relationship w–S_r decreases toward the origin along a different line than for the no complex-crack cases (Cases 1–4). In Cases 5 and 6, which are 'atmospheric-stirred' slurry clay with low w_i, numerous visible bubbles of various sizes are trapped in the specimen. The effect of this is seen in Fig. 5(b) where, before the value of w reaches around w_S, the value of e decreases to meet the S_r = 80% line for Cases 5 and 6, while decreasing along the S_r = 100% line for Cases 1–4. After w drops below w_S, e does not change significantly in any of the cases. The value of e at the end of the test in Cases 5 and 6 (numerous bubbles) is slightly larger than that in Cases 1–4 (few bubbles).

4 CONCLUSIONS

The main conclusions drawn through air-drying tests on slurry clay are as follows.

(1) Visible bubbles influence the form of cracks. Cracks with a more complex geometry form when the initial water content is lower.

(2) In spite of changes in the surface area, the rate of decrease in mass and volume is almost constant from the beginning of drying. Neither initial water content nor crack generation affects this rate.

(3) In every case, the average water content is almost equal to the local water content. Visible bubbles and cracks do not alter the water content change.

(4) The relationships w–S_r and w–e and the value of e at the end of air drying differ depending on the presence of visible bubbles.

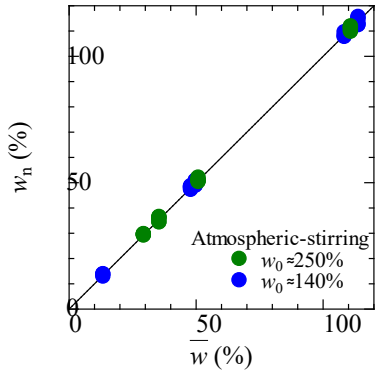

Fig. 4. Horizontal distribution of water content of specimen in air-drying process

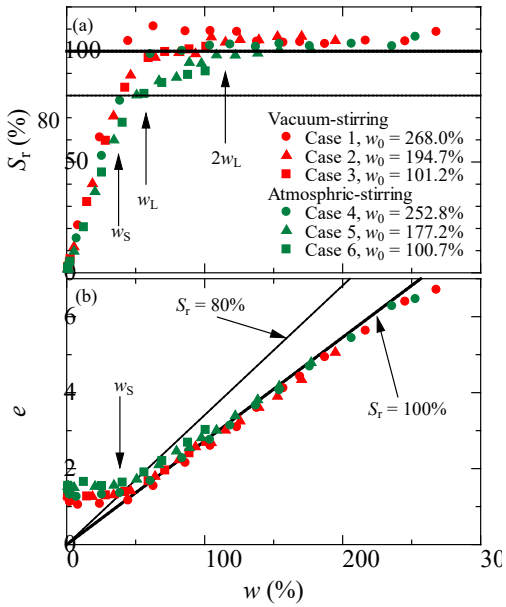

Fig. 5. Relationships w-S_r and w-e

ACKNOWLEDGEMENT

The X-ray CT scanner was presented from RF Co., Ltd. The experiment was carried out as part of graduation research of Mr. Kiyomasa Homma, Formerly of Shinshu University. The authors are deeply grateful to them.

REFERENCES

T. Umezaki & T. Kawamura, 2013, Shrinkage and desaturation properties during desiccation of reconstituted cohesive clay, Soil and Foundations, Vol.53, No.1, pp.47-63.

H. Seya, T. Umezaki & T. Kawamura, 2017, Shrinkage of clay subjected to vacuum evaporation or air drying, In Proceedings of the 52nd Japanese Geotechnical Society Annual Meeting, Japan, pp.327-328 (in Japanese).